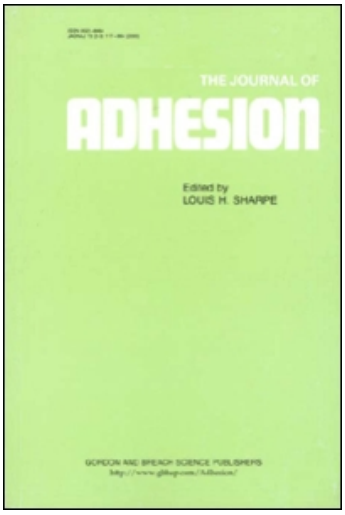

The Journal of Adhesion
Publication details, including instructions for authors and subscription information:
http://www.informaworld.com/smpp/title~content=t713453635

Bumpy Particle Adhesion and Removal in Turbulent Flows Including Electrostatic and Capillary Forces

Goodarz Ahmadi[a]; Shiguang Guo[a]
[a] Department of Mechanical and Aeronautical Engineering, Clarkson University, Potsdam, New York, USA

To cite this Article Ahmadi, Goodarz and Guo, Shiguang(2007) 'Bumpy Particle Adhesion and Removal in Turbulent Flows Including Electrostatic and Capillary Forces', The Journal of Adhesion, 83: 3, 289 — 311
To link to this Article: DOI: 10.1080/00218460701239174
URL: http://dx.doi.org/10.1080/00218460701239174

The Journal of Adhesion, 83:289–311, 2007

ISSN: 0021-8464 print/1545-5823 online
DOI: 10.1080/00218460701239174

Taylor & Francis
Taylor & Francis Group

Bumpy Particle Adhesion and Removal in Turbulent Flows Including Electrostatic and Capillary Forces

Goodarz Ahmadi
Shiguang Guo
Department of Mechanical and Aeronautical Engineering,
Clarkson University, Potsdam, New York, USA

The effect of electrostatic and capillary forces on bumpy particle adhesion and removal in turbulent flows is studied. We use the JKR theory and account for the increase of adhesion by capillary force. The effects of electrostatic forces and nonlinear hydrodynamic drag are included in the analyses. The criteria for incipient rolling and sliding detachments and electrostatic lifting removal are evaluated. A turbulence burst model is used for evaluating the peak air velocity near the substrate. The critical shear velocities for detaching particles of different sizes under different conditions are evaluated. The electric field strength needed for electrostatic removal of particles with different charges is also estimated. The results are compared with those obtained in the absence of the capillary force. Comparisons of the model predictions with the available experimental data are also presented.

Keywords: Adhesion and removal; Bumpy particle; Capillary force; Electrostatics

INTRODUCTION

Particle adhesion and removal are important in a variety of scientific and engineering applications. In particular, removal of fine particles from a surface is of great concern in the semiconductor, pharmaceutical, and xerographic industries. Recently, there has been concern about the contribution of particle resuspension from common flooring to indoor air pollution.

Received 6 March 2006; in final form 17 January 2007.
Address correspondence to Goodharz Ahmadi, Department of Mechanical and Aeronautical Engineering, Clarkson University, Potsdam, NY 13699–5725, USA. E-mail: ahmadi@clarkson.edu

According to the reviews of particle adhesion and removal provided by Corn [1], Krupp [2], Visser [3], Tabor [4], and Bowling [5], the van der Waals force makes the major contribution to the particle adhesion to a surface under dry conditions. The JKR adhesion model developed by Johnson, Kendall, and Roberts [6] includes the effects of the surface energy and surface deformation. Using the Hertzian profile assumption, Derjaguin, Muller, and Toporov [7] developed a particle adhesion theory, which now is referred to as the DMT model. Recent developments on adhesion models were presented by Tsai, Pui, and Liu [8,9], Maugis [10], and Rimai, DeMejo, and Verrland [11]. Additional related articles on particle adhesion may be found in the books edited by Mittal [12], and Quesnel, Rimai, and Sharpe [13].

Detachment of particles from surfaces has been studied by a number of authors. Corn [1] and Corn and Stein [14] measured the re-entrainment of particles from plane surfaces, where the importance of surface roughness and relative humidity was noted. Punjrath and Heldman [15] studied the particle resuspension mechanisms through a series of wind-tunnel experiments. Healy [16], Sehmel [17], Smith, Whicker, and Meyer [18], Hinds [19], and Nicholson [20] provided reviews of resuspension processes. Particle detachment mechanisms in turbulent flows were studied by Cleaver and Yates [21], where a resuspension model based on the turbulence bursts was developed. Additional advances on particle resuspension processes were reported by Reeks and Hall [22], Wen and Kasper [23], Wang [24], Tsai, Pui, and Liu [8,9], and Soltani and Ahmadi [25–28], Ibrahim, Dunn, and Brach [29].

Earlier works were concerned with ideal, smooth spherical particles and smooth surfaces. Real particles, however, are irregular and bumpy. Greenwood and Williamson [30] suggested that the contact deformation depends on the topography of the surface. Greenwood and Tripp [31] improved the Hertz contact model by taking into account the effect of roughness. Soltani and Ahmadi [27] studied the effect of surface roughness on particle detachment mechanisms. Recently, Rimai, Quesnel, and Reirenberger [32] studied the adhesion of irregularly shaped particles to plane substrate. Gotzinger and Peukert [33] studied the effect of particle charge and roughness on particle adhesion.

The resuspension of charged particles is strongly affected by the presence of electric fields. Extensive studies on adhesion of charged particles were reported by Derjaguin and Smilge [34], Davis [35], Kottler, Krupp, and Rabenhorst [36], and Mastrangelo [37]. Donald [38,39] showed the strong dependence of adhesion force on the presence of an external electric field. Goel and Spencer [40] analyzed the effect of electrostatic and van der Waals forces on adhesion of toner

particles. Detachment of charged toner particles under the action of an electric field was studied by Hays [41,42]. The effect of electrostatic forces on the adhesion of electrophotographic toners to photoconductor in xerographic printers was studied by Lee and Jaffe [43]. A set of experiments to quantify the relative contributions of nonelectrostatic and electrostatic forces to the net adhesion force was performed by Mizes [44]. Soltani and Ahmadi [28] evaluated the minimum critical shear velocity needed to remove different size particles, including electrostatic forces.

A number of researchers have shown that the capillary force plays an important role in particle adhesion. Hinds [19] reported the expression for adhesion force at different values of relative humidity. Zimons's [45] experiments indicated that the effect of capillary condensation on adhesion force begins to appear at air relative humidity greater than 50%. Luzhnov [46] performed experiments on factors affecting the capillary forces. Podczeck, Newton, and James [47], Busnaina and Elsawy [48], and Tang and Busnaina [49] reported the results of their study on the effect of relative humidity on particle adhesion and removal. Ahmadi, Guo, and Zhang [50] studied the effect of the capillary force on the minimum critical shear velocities needed for removing different size spherical particles from surfaces.

Many of the particles that are found in indoor environments are relative by compact but generally rough and irregular in shape. As a first step, these particles may be approximated as bumpy particles. Electrostatic effects and capillary forces may also be affecting the particle resuspension process. In this study, the effects of electrostatic and capillary forces on bumpy particle detachment from a plane surface are studied. It is assumed that the charges reside on the particle bumps and that the adhesion force of each bump is governed by the JKR theory. Both the Boltzmann and the saturation particle-charge distributions are considered. The effect of capillary forces acting on the contact bumps–substrate interface is also included. The minimum critical shear velocities required for detaching charged smooth and bumpy particles in the size range of 1 to 60 μm in the presence of capillary force under different conditions are evaluated.

BUMPY PARTICLE ADHESION

Most natural and industrial particles are irregular and bumpy in shape, and adhesion of irregular shaped particles is relatively complex and far from being understood. Soltani and Ahmadi [28] proposed that compact particles with coarse roughness could be modeled as spheres with a number of bumps. A schematic of a bumpy particle is

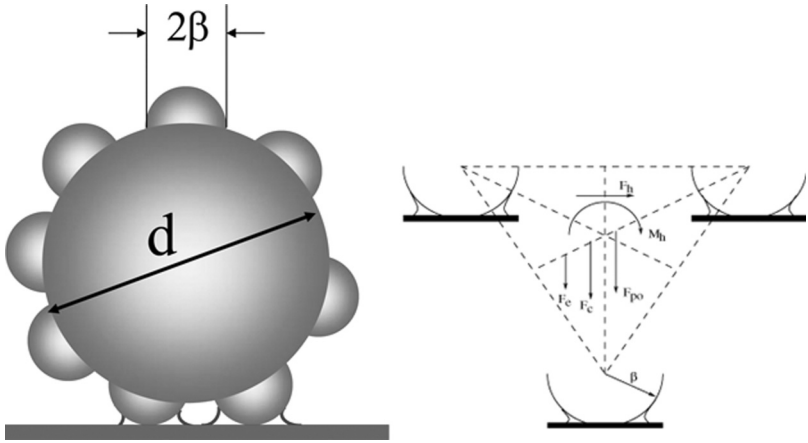

FIGURE 1 Schematic diagram of a bumpy particle and contact bumps in the presence of a capillary meniscus, as well as the contact forces.

shown in Figure 1. The bumps are then approximated to be hemispheres of radius β. The relationship among the radius of the bump β, the number of bumps N, and the particle diameter d is given as

$$\beta = \frac{d}{n_u n_b \sqrt{N}} \tag{1}$$

where $n_b = 1,2,\ldots$ controls the average spacing between the bumps that are in contact with the substrate and n_u is a numerical parameter (greater than 1) used to allow for nonuniform distribution of bumps on the particle surface. (Note that $n_u = 1$ is the limit for a uniform distribution of bumps.)

This bumpy sphere model may be a suitable representation for adhesion of toners in xerographic copiers. It was reported by Goel and Spencer [40] and Hays [41,42] that, on the average, there are three asperities of a toner particle in contact with the substrate. Following Soltani and Ahmadi [28], it is assumed that a particle with coarse surface roughness has three bumps in contact with the substrate. Furthermore, the contact bump centroids are taken to be located at distances of $2n_b\beta$ from each other, whereas the noncontact bumps are on the average $2n_bn_u\beta$ apart.

JKR ADHESION MODEL

In this study, the JKR adhesion model is used to describe the interaction of a hemispherical bump with a plane surface. According

to the JKR model, the pull-off force f_{po} for each bump of radius β that is in contact with the substrate is given as

$$f_{po}^{JKR} = \frac{3}{2}\pi W_A \beta, \tag{2}$$

where W_A is the thermodynamic work of adhesion. The total pull-off force then becomes

$$f_{ad}^{JKR} = \frac{3}{2}\pi N_c W_A \beta \tag{3}$$

where N_c is the number of contact bumps (with $N_c = 3$ representing toner-like particles).

CAPILLARY FORCE

In humid air with relative humidity (RH) higher than 60 to 70%, condensation of water vapor around the particle–substrate contact area forms a meniscus as shown in Figure 1. (Condensation of water vapor in some areas could occur at lower RHs.) When a meniscus is formed, it generates a capillary force that adds to the van der Waals force. When present, the capillary force significantly enhances the adhesion between the particle and the substrate. Here it is assumed that particles are deposited on the surface under dry conditions and then a liquid meniscus forms on the particle–substrate contact. The maximum capillary force for a spherical particle of diameter d is given as

$$f_c = 2\pi\sigma d, \tag{4}$$

where σ is the surface tension of water ($\sigma = 0.0735\,N/m$, at room temperature). The particle flattening effect is assumed to be small, and its potential effect in Equation (4) is neglected.

For irregular particles, it is assumed that the meniscus forms around each bump–substrate contact and, therefore, the capillary force for each contact bump becomes $F_c^B = 4\pi\sigma\beta$. The total capillary force then is given by

$$F_c = 4\pi\sigma\beta N_c \tag{5}$$

Equation (5) assumes that liquid meniscus stays around the bump–substrate contact, and the flattening effect of the bump is negligible. If liquid floods the contact area, submerges the bumps, and forms around the body of particle, Equation (5) is no longer applicable and Equation (4) should be used.

Equations (4) and (5) are for the case that a liquid meniscus is formed. That generally occurs at a high level of RH. The nature of

the surface (hydrophilic or hydrophobic) will also significantly affect the formation of meniscus.

CHARGE DISTRIBUTION

Aerosols could be changed by a variety of mechanisms; some are well understood and others are not fully understood. In this section, the Boltzmann charge distribution and saturation field/diffusion charge distribution, which are used in this study, are outlined.

Boltzmann Charge Distribution

Small particles in a bipolar ionic atmosphere tend toward the Boltzmann charge distribution (Fuchs [51], Hinds [19], and Hidy [52]). For a cloud of particles of diameter d under equilibrium condition at temperature T, the fraction f(n) of particles with n elementary electronic charges is given as

$$f(n) = \frac{e^{(n^2e^2/dkT)}}{\sum_{n=-\infty}^{+\infty} e^{(n^2e^2/dkT)}} \tag{6}$$

where k is the Boltzmann constant ($k = 1.38 \times 10^{-16}$ erg/K, e is the elementary unit of charge ($e = 1.6 \times 10^{-19}$ coulomb in SI units, and $= 4.8 \times 10^{-10}$ statcoulomb in cgs units), and T is the temperature of the gas. The average number of absolute charge per particle is given as

$$\bar{n} = \sum_{n=-\infty}^{+\infty} nf(n). \tag{7}$$

For particles larger than 0.03 μm, the summation in Equation (7) may be approximated as

$$\overline{|n|} \approx 2.37\sqrt{d}, \tag{8}$$

where d is the particle diameter in μm. The average number of positive or negative charges carried by a particle then is $\overline{|n|}/2$. It should be emphasized that the Boltzmann charge distribution is for an ideal condition where aerosols have sufficient time to come to equilibrium with the positive and negative ions of the same concentration.

Diffusion and Field Charging

Small particles also become charged through diffusion and field-charging mechanisms in a unipolar ionic environment. The

approximate number of charges n acquired by a particle of diameter d by diffusion charging during time t is given as [19]

$$n_{diff} = \frac{dkT}{2e^2} \ln\left(1 + \frac{\pi d \bar{c}_i}{2kT} e^2 N_i t\right) \tag{9}$$

where $c_1 = 2.4 \times 10^4$ cm/s is the mean thermal speed of the ions and N_i is the concentration of ions. In the subsequent analysis, a typical value of $N_i t \approx 10^8$ ion $\cdot$ s/cm^3 is used.

In the presence of a strong electric field, the field charging becomes the main charging mechanism. After sufficient time, the saturation number of charges n acquired by a particle is given as [19]

$$n_{field} = \frac{3\varepsilon}{\varepsilon + 2} \frac{Ed^2}{4e}, \tag{10}$$

where ε is the dielectric constant of the particle. Equations (9) and (10) are expressed in cgs units.

On the basis of the earlier studies by Hays [41], in the present study it is assumed that the charges carried by a particle are mainly concentrated on its bumps.

ELECTROSTATIC FORCES

A brief summary of the electrostatic forces used in this study is presented in this section. The force acting on a charged particle near a conducting, infinitely long plane substrate in the presence of an applied electric field, is given approximately as (Hartmann *et al.* [53]; Hidy [52]; Cooper *et al.* [54]; Fan and Ahmadi [55])

$$F_e = qE - \frac{q^2}{16\pi\varepsilon_o y^2} + \frac{qEd^3}{16y^3} - \frac{3}{128} \frac{\pi\varepsilon_o d^6 E^2}{y^4} \tag{11}$$

where $\varepsilon_o = 8.859 \times 10^{-12}$ amp $\cdot$ sec/V $\cdot$ m is the permittivity (dielectric constant of free space), d is the particle diameter, E is the imposed (constant) electric field strength, y is the distance of the center of the spherical particle from the surface, and q is the total charge on the particle. For a particle that carries n units of charge, the total electrical charge is given as

$$q = ne. \tag{12}$$

In Equation (11), the terms on the right-hand side are, respectively, the Coulomb force resulting from the applied electric field, the image force, the dielectrophoretic force and the polarization force. The Coulomb and dielectrophoretic forces can be either toward or away

from the wall, while the image and polarization forces are always directed toward the surface. The dielectrophoretic force depends on the gradient of the electric field and the exact expression is geometry dependent. However, for a charged sphere near a conducting plane substrate in the presence of an imposed constant electric field, the expression given in Equation (11) is a reasonable approximation. Note that in this case the dielectrophoretic force is generated by the gradient of the field from the image charge. An expression for the dielectrophoretic force in a more general situation was described at length by Jones [56]. In this study, the effect of the contact-potential-induced electrical double-layer force for particles in air is neglected.

ELECTROSTATIC FORCES ACTING ON A BUMPY PARTICLE

The electrostatic force acting on a bumpy charged particle was studied by Soltani and Ahmadi [28]. It was assumed that a charged bumpy particle has three bumps in contact with the substrate. Thus, for a uniform charge distribution on the bumps, the charge on each contact hemispherical bump is effectively concentrated at a distance of $\beta/2$ from the substrate. The electrostatic force acting on the charged bumpy particle then is given as

$$F_e = -1.5qE - \frac{q^2}{4\pi\varepsilon_o}\left[\frac{(1-3/N)^2}{d^2} + \frac{[(4n_b^2+1)(3/N)^2]}{3\beta^2(4n_b^2+1)^{3/2}}\right] - 72\pi\varepsilon_o\beta^2E^2. \tag{13}$$

In the derivation of Equation (13) from (11), for the entire charged sphere for the contact bumps, $y = d/2$ and $y = \beta/2$ were used, respectively. The terms on the right-hand side of Equation (13) are, respectively, the combined effect of Coulomb and dielectrophoretic forces, the image force, and the polarization force. (In the following sections, the combined force is referred to as the Coulomb force for short.) Unless stated otherwise, all the electrostatic forces are assumed to be directed toward the wall for evaluating the maximum force acting on the particle.

Potential variation of the distribution of electrostatic charges on the particle bump due to the presence of a liquid meniscus was not addressed in this study. In the subsequent analysis, we assumed that the charge distribution is not affected by the formation of a liquid meniscus.

HYDRODYNAMIC FORCES AND TORQUE

The near-wall turbulent flow is dominated by vortical coherent structures and occasional bursts, which have profound effects on the

particle detachment process [25–27]. In this article, the burst model for particle resuspension is used.

The maximum instantaneous streamwise velocity experienced locally near the wall during the turbulent burst/inrush is given in wall units as [27]

$$u_M^+ = 1.72y^+, \tag{14}$$

where a superscript $+$ denotes a quantity stated in wall units. That is,

$$u^+ = \frac{u}{u^*}, \qquad y^+ = \frac{yu^*}{\nu}, \tag{15}$$

where ν is the kinematic viscosity of the fluid and u^* is the shear velocity.

The hydrodynamic drag force acting on a spherical particle that is in contact with a smooth wall may be expressed as

$$F_h = \frac{C_D \pi f \rho_g d^2 V^2}{C_c}, \tag{16}$$

where C_c is the Cunningham slip correction factor, $f = 1.7009$ is the correction factor for the wall effect given by O'Neil [57], ρ_g is the air density at normal conditions, V is the mean air velocity at the centroid of the sphere, and C_D is the drag coefficient.

The drag coefficient is given as [19]

$$C_D = \begin{cases} \frac{24}{Re}(1 + \frac{1}{6}Re^{2/3}) & \text{for } Re \le 1000, \\ 0.44 & \text{for } 1000 \le Re \le 2 \times 10^5. \end{cases} \tag{17}$$

Note that, in earlier works, the linear Stokes drag was used in evaluating the hydrodynamic forces acting on particles. However, when the capillary and electrical forces are present, the required removal velocity may become quite large. With the particle Reynolds number increasing, the effect of nonlinear drag as described by Equation (17) becomes important.

The hydrodynamic torque is given by

$$M_h = \frac{2\pi\mu f_m d^2 V}{C_c} \tag{18}$$

where $f_m = 0.943993$ is the wall effect correction factor given by O'Neil [57]. In this work, it is assumed that the hydrodynamic drag and torque acting on the bumpy particle in contact with a surface are given by Equations (16) and (18).

DETACHMENT MODELS

In this section, brief summaries of rolling, sliding, and electrical lifting detachment are presented.

Rolling Detachment Model

In this section, a rough particle with three bumps in contact with a plane smooth surface is studied. Figure 1 shows the schematic of the forces acting on the particle and their lines of action. The particle could be removed by breakup of one of the contact bumps and rolling with respect to the axis formed by connecting the centers of the other two contact bumps. It is assumed that the direction of the hydrodynamic drag force is perpendicular to the corresponding rolling axis. The onset of detachment with respect to a rolling axis (centerline of two bumps) is determined by the balance of torques generated by external and resistance forces, that is,

$$M_h + F_h \frac{d}{2} \geq (F_{ad} + F_e + F_c)(0.58 n_b \beta), \tag{19}$$

where F_{ad} is the pull-off force for the bumpy particle with three bumps in contact with the substrate as given by Equation (3). It is assumed that the adhesion force at the moment of incipient rolling is equal to the pull-off force. Because of symmetry, the lines of the action of adhesion force, capillary force, and the electrical forces are located at the centroid of the triangle that connects the centers of the hemispherical bumps as shown in Figure 1. The effect of the hydrodynamic lift force in Equation (19), which is expected to be small, is neglected.

Sliding Detachment Model

Wang [24] and Soltani and Ahmadi [25] studied the particle sliding detachment process. Accordingly, when the external force parallel to the surface becomes larger than the friction force, the particle will be removed by sliding. When the effect of the electrical force and the capillary force is included, the condition for sliding detachment of the particle becomes

$$F_h \geq k(F_{ad} + F_c + F_e) \tag{20}$$

where k is the coefficient of static friction for the particle–surface interface. Here, also, the effect of the hydrodynamic lift force is neglected. Here, a simple Coulomb model for the friction force is

assumed, and the microscopic detail of the friction force, which is believed to be related to the adhesion hysteresis, is not addressed.

Electrostatic Particle Detachment

The electrostatic detachment is the main mechanism used in the transfer of toner between surfaces in xerographic copiers. In the absence of hydrodynamic forces, the onset of list-off of a charged particle from a substrate is controlled by the balance of the adhesion force, the electrical forces and the capillary force normal to the surface. Accordingly, the particle will be detached by electrostatic lifting if

$$F_{ec} + F_{ed} \geq F_{ad} + F_{ei} + F_{ep} + F_c, \tag{21}$$

where $F_{ec}, F_{ed}, F_{ei}, F_{ep}$, respectively, stand for the standard electrostatic (qE), dielectrophoretic, image, and polarization forces.

RESULTS AND DISCUSSION

In this section, results concerning the critical shear velocities for bumpy particle removal in humid and dry turbulent airflow are presented. For humid air, it was assumed that the RH is higher than 60% to 70% so that the meniscus is formed and Equation (4) is applicable. Unless stated otherwise, detachment of a polystyrene particle from a polystyrene substrate is analyzed. The corresponding material properties are listed in Table 1.

Figure 2 shows variations of the critical shear velocity with diameter for resuspension of neutral bumpy particles with and without capillary force for different detachment mechanisms. Here, it is assumed that the particle has 20 bumps and that the contact bumps are one bump diameter apart (*i.e.*, $n_b = 2$); $n_u = 2$ and Equation (1) are used to evaluate the bump radius. The near wall velocity variation was evaluated with the use of Equation (14). The critical shear velocity is quite high for small particles and decreases sharply as d increases. The capillary force increases the critical shear velocity for removal of these bumpy particles by roughly a factor of two to three. Figure 2 also shows that the critical shear velocities for sliding detachment with and without capillary force are higher than those for the rolling detachment. Thus, these particles are generally removed by the rolling mechanism. The effects of number of bumps on the critical shear velocities for resuspension of neutral particles with and without capillary force are shown in Figure 3. The results for smooth particles are also reproduced in this figure for comparison. Here, the rolling removal mechanism is considered, it is assumed that the contact bumps are

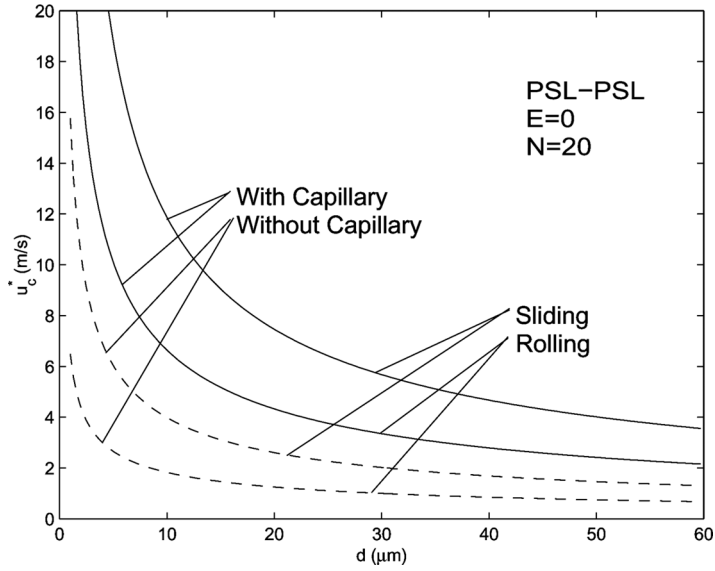

FIGURE 2 Variations of critical shear velocity with particle diameter for resuspension of neutral polystyrene particles from a polystyrene substrate, with and without capillary force, for different detachment mechanisms.

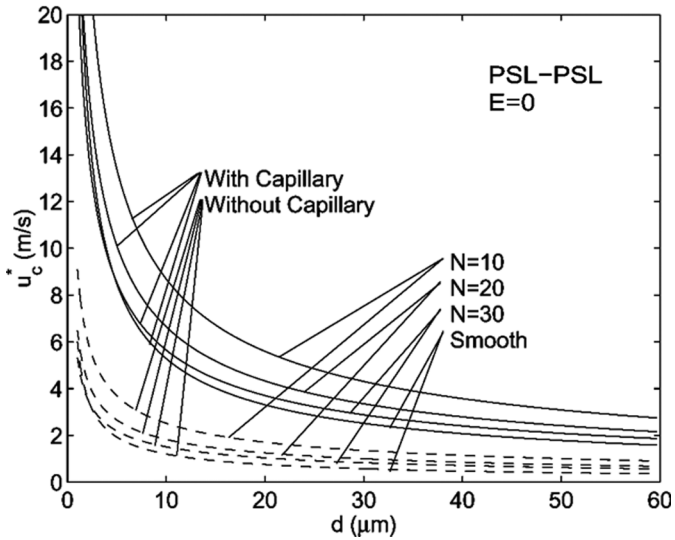

FIGURE 3 Variations of critical shear velocity with particle diameter for resuspension of neutral polystyrene particles from a polystyrene substrate, with and without capillary force, for smooth and bumpy particles.

one diameter apart (*i.e.*, $n_b = 2$), and $n_u = 2$ is used. It is observed that the critical shear velocities in the presence of capillary force are higher than those obtained in the absence of capillary force for both smooth and bumpy particles. In particular, the capillary generates the dominant component of the adhesion force for both smooth and bumpy particles smaller than 10 μm. Figure 3 also shows that the critical shear velocity increases as the number of bump decreases (*i.e.*, when the particle becomes more irregular, in that it has a smaller number of large bumps).

Figure 4 shows variations of the critical shear velocity with diameter for resuspension of particles that carry the saturation charge with and without capillary force in the presence of an electric field intensity of $E = 5000\,kV/m$. Results for smooth and bumpy particles (with different number of bumps) are shown in this figure. Here, it is assumed that particles are removed by rolling, and $n_u = 2$ is used. The critical shear velocities in the presence of capillary force are higher than those in its absence. Comparison of Figures 3 and 4 shows that the electrostatic forces significantly increase the adhesion forces of both smooth and bumpy particles. As a result, the critical shear velocities needed to

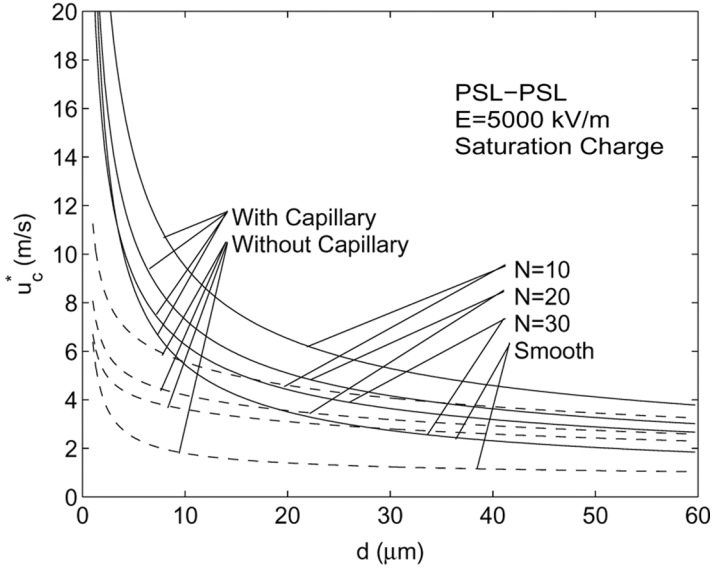

FIGURE 4 Variations of critical shear velocity with particle diameter for resuspension of polystyrene particles with saturation charge from a polystyrene substrate, with and without capillary force, for smooth and bumpy particles.

remove the particle increase accordingly. The relative increase of the critical shear velocity due to the capillary in the presence of the electrostatic forces is not as large as that for the neutral particle. This further indicates the importance of electrostatic forces on particle adhesion.

A similar study for removal of particles that have the Boltzmann charge distribution is also performed. Figure 5 shows variations of critical shear velocity with particle diameter for resuspension of polystyrene particles with the Boltzmann charge distribution from a polystyrene substrate, with and without capillary force, for smooth and bumpy particles. Here, it is assumed that an electric field strength of 5000 kV/m is present, and different numbers of bumps are considered. The effects of the electrostatic force become negligibly small, and the critical shear velocities become almost the same as those shown in Figure 3 for a neutral particle.

Figure 6 shows variations of critical shear velocity with particle diameter for resuspension of particles with a 20 μC/gm charge, with and without capillary force, for smooth and bumpy particles. This corresponds to a typical amount of charge carried by the toner particles in

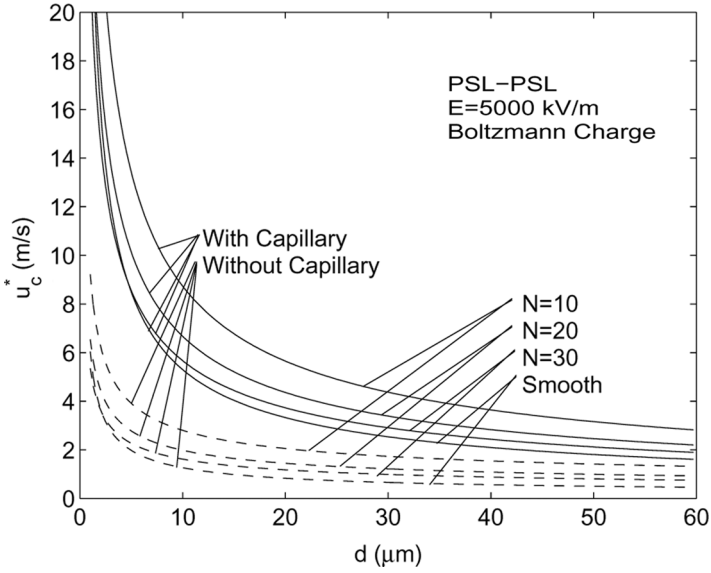

FIGURE 5 Variations of critical shear velocity with particle diameter for resuspension of polystyrene particles with Boltzmann charge from a polystyrene substrate, with and without capillary force, for different values of nonuniformity.

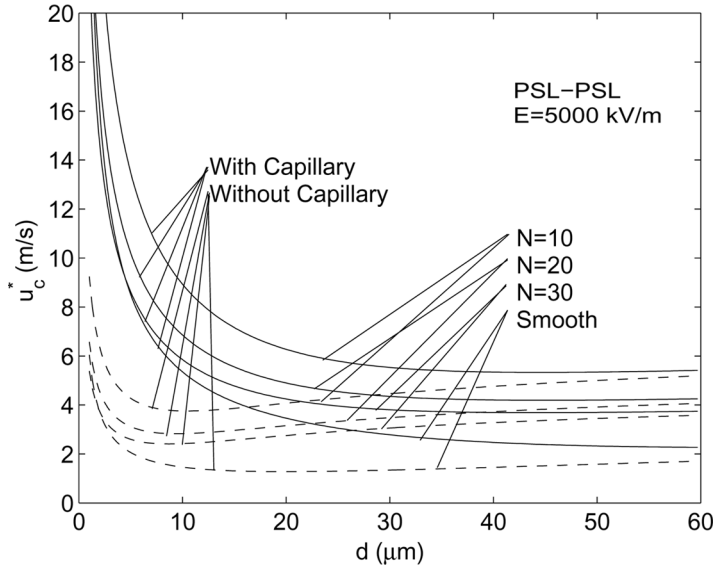

FIGURE 6 Variations of critical shear velocity with particle diameter for resuspension of polystyrene particles with saturation charge from a polystyrene substrate, with and without capillary force, for smooth and bumpy particles.

xerographic copiers. Here, it is assumed that the contact bumps are one diameter apart (*i.e.*, $n_b = 2$), and $n_u = 2$ is used. In the absence of capillary effects, the critical shear velocity decreases sharply with d to a minimum value and then increases slightly with further increase in particle diameter. The effect is more noticeable for bumpy particles. A similar variation was noted earlier by Soltani and Ahmadi [28]. When capillary forces are present, there is a monotonic decrease of u_c^* with d. For particles less than 30 μm, it is observed that the critical velocities in the presence of capillary force are higher that those in its absence. The effect of capillary force on removal velocity is not significant for particle diameter larger than 30 μm. This is because the electrical forces provide the dominant contribution to the adhesion force for these relatively large particles.

Figure 7 shows variations of the critical shear velocity with particle diameter for resuspension of a neutral bumpy particle, with and without capillary force, for different values of nonuniformity parameter, n_u. Here, it is assumed that the contact bumps are one diameter apart (*i.e.*, $n_b = 2$), and $N = 20$ bumps are present. The critical shear velocities for $n_u = 1$ are higher than those for $n_u = 2$ in the presence or

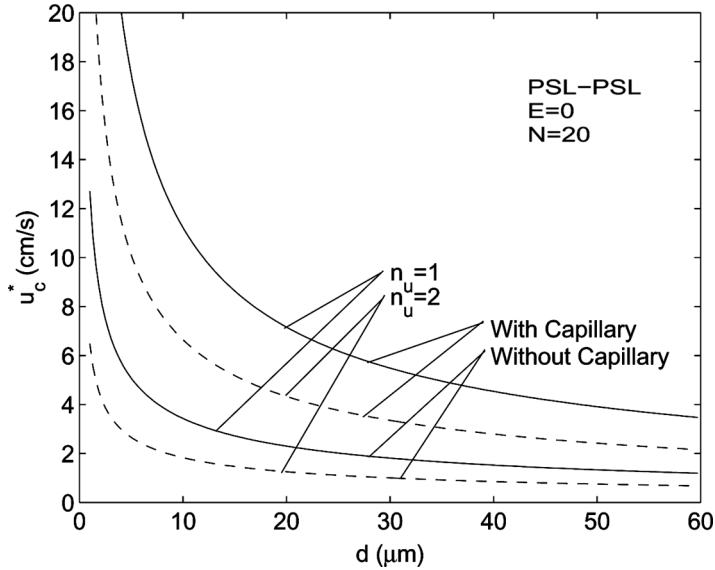

FIGURE 7 Variations of critical shear velocity with particle diameter for resuspension of neutral polystyrene particles from a polystyrene substrate, with and without capillary force, for different values of nonuniformity.

absence of capillary force. This is because both van der Waals and capillary forces as given by Equations (3) and (5) are directly proportional to the bump radius, β. As n_u increases, Equation (1) shows that the bump radius decreases. Thus, the net adhesion force decreases and the corresponding critical shear velocity for particle removal decreases. For n_u equal to 1 and 2, Table 2 shows the bump radii, the adhesion forces, and the capillary forces acting on a bumpy 30-μm polystyrene particle in contact with a polystyrene substrate. When the nonuniformity factor is double the bump radius, the adhesion and capillary forces are reduced by a factor of two.

Figure 8 shows variations of the critical shear velocity with particle diameter for resuspension of bumpy particles with saturation

TABLE 1 Material Properties

Material	E (10^8 N/m^2)	A (10^{-20} J)	W_A (10^{-3} J/m^2)	ρ_g (10^3 Kg/m^3)	v_i	k
PSL-PSL	28	6.37	10.56	1.05	0.33	0.5
PSL-Nickel	—	14.27	23.65	—	—	—

TABLE 2 Magnitude of Forces for a Bumpy 30-μm Polystyrene Particle in Contact with a Polystyrene Substrate in the Presence of an Electric Field of 5000 kV/m

n_u	β (m)	F_u (N)	F_c (N)	F_{Coul} (N)	F_{Imag} (N)	F_{Pola} (N)
1	3.35×10^{-6}	5.0×10^{-7}	9.2×10^{-6}	1.8×10^{-6}	8.35×10^{-7}	5.6×10^{-7}
2	1.67×10^{-6}	2.5×10^{-7}	4.6×10^{-6}	1.8×10^{-6}	1.9×10^{-6}	1.4×10^{-7}

charge, with and without capillary force, for different values of nonuniformity, n_u. An electric field intensity of $E = 5000$ kV/m is assumed to be present. Similar to Figure 7, the critical shear velocities for $n_u = 1$ are higher than those for $n_u = 2$ in the presence or absence of capillary force. By comparing Figures 7 and 8, it is also observed that the effect of the nonuniformity factor in the absence of electrostatic force is more significant than that in its presence.

The electrostatic forces acting on a 30-μm polystyrene particle under an electrical field intensity of 5000 kV/m are listed in Table 2. Here, F_{Coul} is the combination of Coulomb and dielectrophoretic forces,

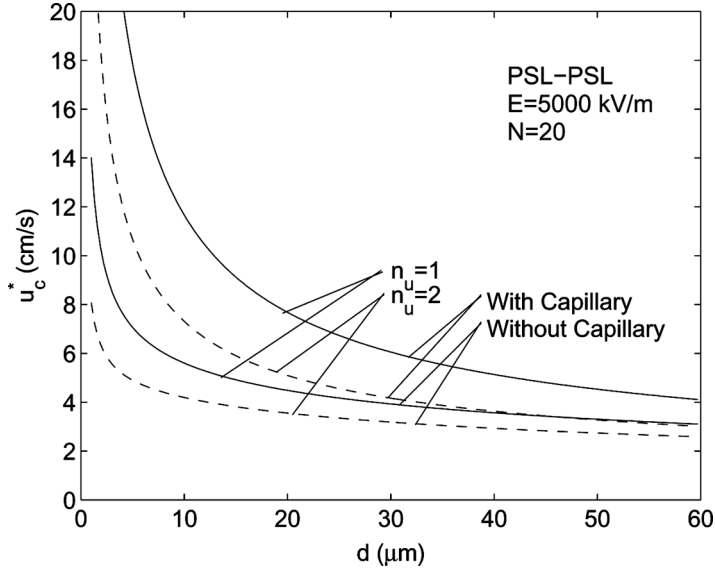

FIGURE 8 Variations of critical shear velocity with particle diameter for resuspension of polystyrene particles with saturation charge from a polystyrene substrate, with and without capillary force, for different values of nonuniformity.

F_{imag} is the image force, and F_{pola} is the polarization force. These correspond, respectively, to the three terms on the right-hand side of Equation (13). Clearly, the Coulomb force (including the dielectrophoretic force) is independent of bump radius, whereas the polarization force is proportional to β^2, and the image force increases with β^{-2}. Therefore as n_u increases and bump radius decreases, the image force increases, and the polarization force decreases, while the Coulomb force remains fixed. Table 2 shows that the image force increases substantially and becomes comparable with Coulomb force. Nevertheless, the net adhesion force decreases as n_u increases from 1 to 2. For rolling detachment, Equation (19) also shows that the resistance moment is also directly proportional to β, which leads to decrease of n_c^* as bump radius decreases (u_u increases).

Variations of the critical shear velocity with particle diameter for resuspension of neutral bumpy particles, with and without capillary force, for different values of average spacing, n_b, are shown in Figure 9. Here, $n_u = 2$ and $N = 20$ are used. The critical shear velocities for $n_b = 1$ are higher than those for $n_b = 2$ in the presence or absence of capillary force. The trend of variation of n_c^* in Figure 9 is quite

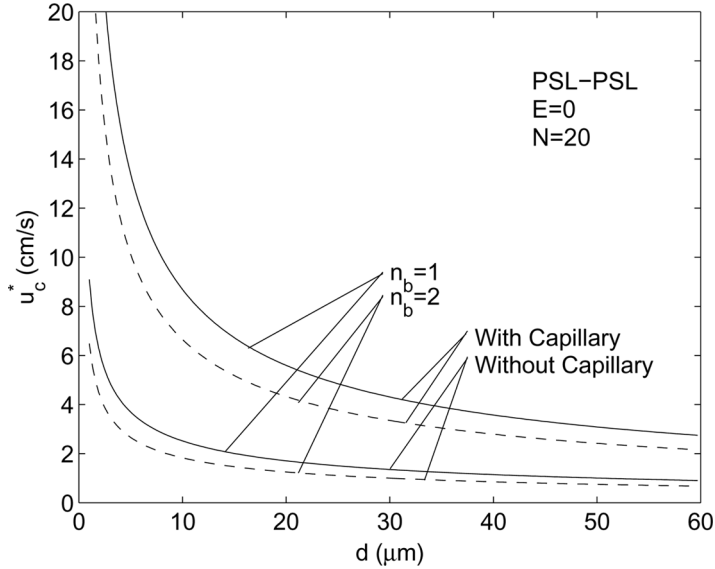

FIGURE 9 Variations of critical shear velocity with particle diameter for resuspension of neutral polystyrene particles from a polystyrene substrate, with and without capillary force, for different values of n_b.

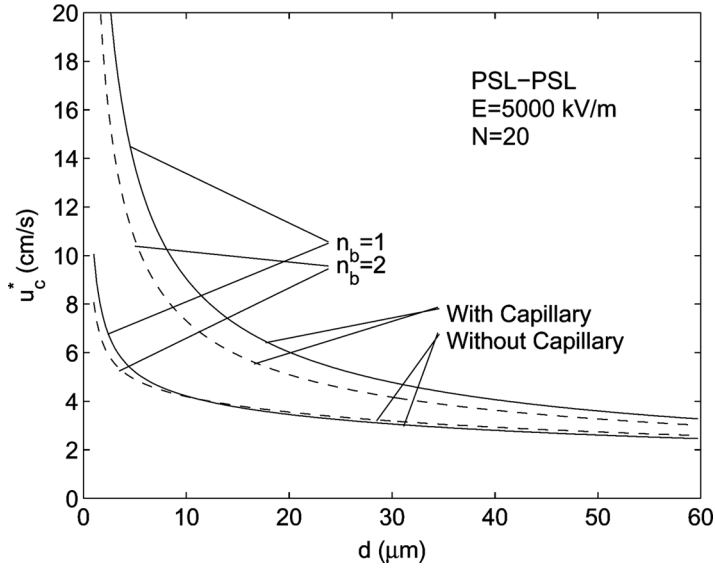

FIGURE 10 Variations of critical shear velocity with particle diameter for resuspension of polystyrene particles with saturation charge from a polystyrene substrate, with and without capillary force, for different values of n_b.

similar to that in Figure 7. Similarly, as u_b increases, the bump radius decreases and thus the adhesion and capillary forces are reduced.

Figure 10 shows variations of the critical shear velocity with particle diameter for resuspension of bumpy particles with saturation charge, with and without capillary force, for different values of n_b. An electric field intensity of $E = 5000\,kV/m$ is assumed to be present. Similar to Figure 9, the critical shear velocities for $n_b = 1$ are generally higher than those for $n_b = 2$ for particles greater than $10\,\mu m$. In the absence of capillary effects and for $d < 10\,\mu m$, however, the critical shear velocity decreases as n_b increases from 1 to 2.

For several values of n_b, the magnitude of forces for a 30-μm particle that carries the saturation charge in the presence of an electric field intensity of $5000\,kV/m$ are listed in Table 3. The numbers in the first two rows of Table 3 are identical to those in Table 2. The exception is the image force for $n_b = 1$, which is different from that for $n_u = 1$. The adhesion, the capillary, and the polarization forces decrease as n_b increases. The Coulomb force is independent of n_b, and the image force increases sharply with n_b. Depending on the amount of charge and the particle size, the increase in electrical image force could become larger than the decrease in the adhesion force; therefore, the net adhesion

TABLE 3 Magnitude of forces for a Bumpy 30-μm Polystyrene Particle in Contact with a Polystyrene Substrate in the Presence of an Electric field on 5000 kV/m

n_u	β (m)	F_{ad} (N)	F_c (N)	F_{Coul} (N)	F_{imag} (N)	F_{pola} (N)
1	3.35×10^{-6}	5.0×10^{-7}	9.2×10^{-6}	1.8×10^{-6}	8.35×10^{-7}	5.6×10^{-7}
2	1.67×10^{-6}	2.5×10^{-7}	4.6×10^{-6}	1.8×10^{-6}	1.9×10^{-6}	1.4×10^{-7}
3	1.12×10^{-6}	1.7×10^{-7}	3.1×10^{-6}	1.8×10^{-6}	3.8×10^{-6}	6.3×10^{-8}
4	8.4×10^{-7}	1.3×10^{-7}	2.3×10^{-6}	1.8×10^{-6}	6.4×10^{-6}	3.5×10^{-8}

force may increase as n_b increases. This trend of variation is seen in Figure 10 for particles larger than 10 μm in the absence of capillary force. When the capillary force is present, it will dominate the net adhesion force for $n_b \leq 2$, and u_c^* decreases with increasing n_b. For n_b equal to 3 and 4, Table 3 shows that the image force makes the largest contribution to the net adhesion force (including capillary) under the stated conditions.

Hays [41] presented a set of experimental data for electrical detachment of toner particles from nickel carrier beads with an average

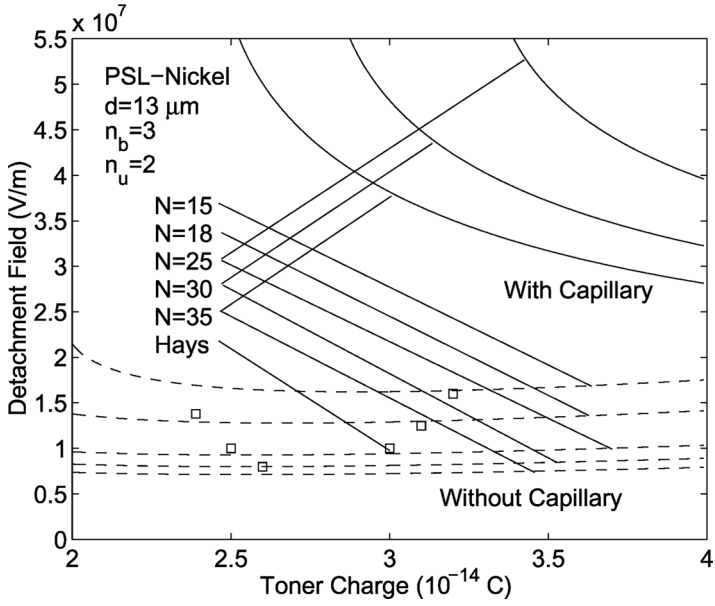

FIGURE 11 Comparison of electric detachment fields for bumpy particles with and without capillary force with the experimental data of Hays [41] for toner particles on a nickel carrier beads.

charge of 3×10^{-14} C. Soltani and Ahmadi [28] showed that the computed electric fields for detaching the toners based on the bumpy particle model are comparable with the experimental data of Hays [41]. For a range of toner charge, Figure 11 compares the computed electric detachment fields for bumpy particles, with and without the capillary force, with the experimental data of Hays. Equation (21) is used, and the material properties for the polystyrene–nickel interface are listed in Table 1. The detachment electric field increases significantly as a result of the presence of the capillary force. Furthermore, the electric field intensity for particle detachment increases with the increase of the toner charge when the capillary force is present. In addition, the critical electric field intensity decreases with the increase of number of bumps in the presence or absence of the capillary force. Figure 11 also shows that the predicted detachment electric fields in the absence of capillary force are in reasonable agreement with the experimental data (Soltani and Ahmadi [28]) for number of bumps in the range of 15 to 35. Although a precise number of bumps for toner particles fitted to spheres is not known, $15 < N < 35$ is within the expected range.

CONCLUSIONS

In this work, resuspension of bumpy particles from surfaces in turbulent flows, including electrostatic and capillary forces, is studied. The hydrodynamic forces and torque acting on the particle along with the adhesion force, capillary force, and electrostatic forces are evaluated. The critical shear velocities and the critical electric field needed to detach different sizes of particles are evaluated. Based on the results presented, the following conclusions may be drawn:

- Rolling is the dominant detachment mode for spherical and bumpy particles in the presence (or absence) of capillary force.
- The capillary effect significantly enhances the particle adhesion force, for both smooth and bumpy particles, and the critical shear velocity for particle resuspension increases accordingly.
- The critical shear velocity increases as the number of bumps decreases. That is, higher velocities are needed to remove the particles that have a smaller number of large bumps.
- The importance of capillary force on the critical removal shear velocity decreases as particle diameter increases (beyond 30 μm).
- As the nonuniformity factor, n_u, increases, the critical shear velocity for removing particles in the presence or absence of the capillary and electrostatic forces decreases.

- The increase of the average bump spacing, n_b, leads to lower critical shear velocity for removal of neutral particles with and without the presence of capillary force.
- For charged particles, in the absence of capillary force, the increase of average bump spacing, n_b, reduces the critical shear velocity for small particles but increases it for larger particles.

ACKNOWLEDGMENTS

The financial support of the Environmental Protection Agency (EPA) and the NYSTAR Center of Excellence is gratefully acknowledged.

REFERENCES

[1] Corn, M., in *Aerosol Science*, C. N. Davies (Ed.) (Academic Press, New York, 1966).
[2] Krupp, H., *Adv. Colloid Interface Sci.* **1**, 111–140 (1967).
[3] Visser, J., in *Surface and Colloid Science*, E. Matijevic (Ed.) (Plenum Press, New York, 1976), Vol. 8, pp. 3–84.
[4] Tabor, D., *J. Colloid Interface Sci.* **58**, 2–13 (1977).
[5] Bowling, R. A., *J. Electrochem. Soc.* **132**, 2208–2219 (1985).
[6] Johnson, K. L., Kendall, K., and Roberts, A. D., *Proc. Royal. Soc. Lond., A* **324**, 301–313 (1971).
[7] Derjaguin, B. V., Muller, V. M., and Toporov, Y. P. T., *J. Colloid Interface Sci.* **53**, 314–326 (1975).
[8] Tsai, C. J., Pui, D. Y. H., and Liu, B. Y. H., *J. Aerosol Sci. Technol.* **15**, 239–255 (1991).
[9] Tsai, C. J., Pui, D. Y. H., and Liu, B. Y. H., *J. Aerosol Sci. Technol.* **22**, 737–746 (1991).
[10] Maugis, D., *J. Colloid Interface Sci.* **150**, 243–269 (1992).
[11] Rimai, D. S., DeMejo, L. P., and Verrland, W., *J. Appl. Phys.* **71**, 2253–2258 (1992).
[12] Mittal, K. L., Ed., *Particles on Surfaces: Detection, Adhesion and Removal* (Plenum Press, New York, 1988, 1989, 1991), Vols. 1–3.
[13] Quesnel, D. J., Rimai, D. S., and Sharpe, L. H., Eds., *Particle Adhesion: Applications and Advances* (Taylor and Francis, New York, 2001).
[14] Corn, M. and Stein, F., *J. Am. Ind. Hyg. Assoc.* **26**, 325–336 (1965).
[15] Punjrath, J. S. and Heldman, D. R., *J. Aerosol Sci.* **3**, 429–440 (1972).
[16] Healy, J. W., in *A Review of Resuspension Models in Transuranics in Natural Environments*, M. G. White and P. B. Dunaway (Eds.) (USERDA, Las Vegas, 1977), pp. 211–222.
[17] Sehmel, G. A., *Environment Intl.* **4**, 107–127 (1980).
[18] Smith, W. J., Whicker, F. W., and Meyer, H. R., *Nuclear Safety* **23**, 685–699 (1982).
[19] Hinds, W. C., *Aerosol Technology, Properties, Behavior and Measurement of Airborne Particles* (John Wiley and Sons, New York, 1982).
[20] Nicholson, K. W., *Atmospheric Environment*, **22**, 2639–2651 (1988).
[21] Cleaver, J. W. and Yates, B., *J. Colloid Interface Sci.* **44**, 464–474 (1973).
[22] Reeks, M. W. and Hall, D., *J. Fluid Eng.* **110**, 165–171 (1988).
[23] Wen, H. Y. and Kasper, J., *J. Aerosol Sci.* **20**, 483–498 (1989).
[24] Wang, H. C., *Aerosol Sci. Technol.* **13**, 386–396 (1990).

[25] Soltani, M. and Ahmadi, G., *J. Adhesion Sci. Tech.* **8**, 763–785 (1994).
[26] Soltani, M. and Ahmadi, G., *J. Adhesion* **51**, 105–123 (1995).
[27] Soltani, M. and Ahmadi, G., *Phys. Fluids* **7A**, 647–657 (1995).
[28] Soltani, M. and Ahmadi, G., *J. Adhesion Sci. Technol.* **13**, 325–355 (1999).
[29] Ibrahim, A. H., Dunn, P. F., and Brach, R. M., *J. Aerosol Science* **34**, 765–782 (2003).
[30] Greenwood, J. A. and Williamson, J. B. P., *Proc. Roy. Soc. Lond. A* **295**, 300–319 (1966).
[31] Greenwood, J. A. and Tripp, J. H., *J. Appl. Mech.* **67**, 153–159 (1967).
[32] Rimai, D. S., Quesnel, D. J., and Reirenberger, R., in *Particle Adhesion: Applications and Advances*, D. J. Quesnel, D. S. Rimai, and L. H. Sharpe (Eds.) (Taylor and Francis, New York, 2001), pp. 283–299.
[33] Gotzinger, M. and Peukert, W., *Powder Technology* **135–136**, 82–91 (2003).
[34] Derjaguin, B. V. and Smilge, V. P., *J. Appl. Phys.* **38**, 4609–4616 (1967).
[35] Davis, D. K., *J. Phys. D: Appl. Phys.* **6**, 1017–1029 (1973).
[36] Kottler, W., Krupp, H., and Rabenhorst, H., *Z. Angew. Phys.* **24**, 219–223 (1968).
[37] Mastrangelo, C. J., *Photogr. Sci. Eng.* **26**, 194–197 (1982).
[38] Donald, D. K., *J. Appl. Phys.* **40**, 3013–3019 (1969).
[39] Donald, D. K., in *Recent Advances in Adhesion*, L. H. Lee (Ed.) (Gordon and Breach, New York, 1973).
[40] Goel, N. S. and Spencer, P. R., in *Adhesion Science and Technology, Part B*, L. H. Lee (Ed.) (Plenum Press, New York, 1975), pp. 763–829.
[41] Hays, D. A., *Photogr. Sci. Eng.* **22**, 232–235 (1978).
[42] Hays, D. A., *Institute of Physics Series No. 66* (The Institute of Physics, London, 1983), p. 237.
[43] Lee, M. H. and Jaffe, A. B., *Particles on Surfaces 1: Detection, Adhesion, and Removal*, K. L. Mittal (Ed.) (Plenum Press, New York, 1988), pp. 169–177.
[44] Mizes, H. A., *J. Adhesion Sci. Technol.* **8**, 937–953 (1994).
[45] Zimon, A. D., *Adhesion of Dust and Powder* (Consultants Bureau, New York, 1982).
[46] Luzhnov, Y. M., *Research in Surface Forces* (Consultants Bureau, New York, 1971).
[47] Podczeck, F., Newton, J. M., and James, M. B., *J. Colloid Interface Science* **187**, 484–491 (1997).
[48] Busnaina, A. A. and Elsawy, T., in *Particle Adhesion: Applications and Advances*, D. J. Quesnel, D. S. Rimai, and L. H. Sharpe (Eds.) (Taylor and Francis, New York, 2001), pp. 391–409.
[49] Tang, J. and Busnaina, A. A., in *Particle Adhesion: Applications and Advances*, D. J. Quesnel, D. S. Rimai, and L. H. Sharpe (Eds.) (Taylor and Francis, New York, 2001), pp. 411–419.
[50] Ahmadi, G., Guo, S., and Zhang, X., *J. Particulate Science Technology* **25**, 59–76 (2007).
[51] Fuchs, N. A., *The Mechanics of Aerosols* (Pergamon Press, Oxford, 1964).
[52] Hidy, G. M., *Aerosol, An Industrial and Environmental Science* (Academic Press, New York, 1984).
[53] Hartmann, G. C., Marks, L. M., and Yang, C. C., *J. Appl. Phys.* **47**, 5409–5420 (1976).
[54] Cooper, D. W., Peters, M. H., and Miller, R. J., *J. Aerosol Sci.* **11**, 133–143 (1989).
[55] Fan, F. G. and Ahmadi, G., *Aerosol Science and Technology* **21**, 49–71 (1994).
[56] Jones, T. B., *Electromechanics of Particles* (Cambridge University Press, Cambridge, UK, 1995).
[57] O'Neill, M. E., *Chem. Eng. Sci.* **23**, 1293–1298 (1968).